Supporting information

Photo-nanozyme Coupling Catalyzes Glucose Oxidation for High-performance Enzymatic Biofuel Cells

Dandan Hu, [1] *Qiwen Su,* [1] *Yan Gao,* [1]*Jian-Rong Zhang,* [1*] *Linlin Wang,* [2*] *and Jun-Jie Zhu* [1*]

[1]State Key Laboratory of Analytical Chemistry for Life Science, School of Chemistry and Chemical Engineering, Nanjing University, Nanjing 210023, P. R. China. E-mail: jrzhang@nju.edu.cn; jjzhu@nju.edu.cn

[2] Shaanxi Key Laboratory of Chemical Additives for Industry, College of Chemistry and Chemical Engineering, Shaanxi University of Science and Technology, Xi'an 710021, China. E-mail: wanglinlin@sust.edu.cn

1 Experimental Section

1.1. Materials and Characterization

All chemicals were of analytical grade and were used as purchased without further purification. Fluorine-doped tin oxide (FTO) substrates (F: SnO_2, ＜15 Ω per square) was obtained from Zhuhai Kaivo Optoelectronic Technology Co., Ltd. Bismuth nitrate pentahydrate (Bi $(NO_3)_3 \cdot 5H_2O$), glucose, disodium hydrogen phosphate dodecahydrate ($Na_2HPO_4 \cdot 12H_2O$), sodium dihydrogen phosphate dihydrate ($NaH_2PO_4 \cdot 2H_2O$), nitric acid (HNO_3, 69%), acetone, ethanol, gold chloride trihydrate ($HAuCl_4 \cdot 3H_2O$) were purchased from Sinopharm Chemical Reagent Co., Ltd. (China). Vanadyl acetylacetonate (VO $(acac)_2$, 99%), 2, 2'-casino-bis (3-ethylbenzothiazoline-6-sulfonic acid) (ABTS), dimethyl sulfoxide (DMSO), polytetrafluoroethylene (PTFE), 1-pyrene butanoic acid succinimidyl ester (PBSE) and p-benzoquinone were obtained from Aladdin Co., Ltd (Shanghai, China). 3,5-dinitro salicylic acid was obtained from Meryer Co., Ltd. Potassium iodide was purchased from Sigma-Aldrich Co., Ltd. Bilirubin oxidase (E.C. 1.3.3.5, from Myrothecium verrucaria, activity ≥ 5 U/mg) was obtained from Nanjing Duly Biotechnology Co., Ltd. Nafion perfluorinated resin solution was purchased from Macklin Reagent Co., Ltd. High-purity single-walled carbon nanotubes (SWCNTs) was purchased from Suzhou Tanfeng Tech Reagent Co., Ltd. Carbon cloth was purchased from Suzhou Sinero Technology Co., Ltd. Ultrapure fresh water obtained from a Millipore water purification system (≥ 18 MΩ, Milli-Q, Millipore) was used throughout the whole experiment.

The UV-vis diffuse reflectance spectra were recorded on a spectrophotometer (Shimadzu UV-3600, Japan) with fine $BaSO_4$ powder as a reference. Fourier-transform infrared (FTIR) spectra were recorded on a Thermo Fisher Nicolet iS50 spectrophotometer. PL emission spectra were measured with an F-7000 spectrophotometer (Hitachi, Japan). Scanning electron microscopy (SEM) images and energy dispersive X-ray spectroscopy (EDS) mapping were obtained by an S-4800 scanning electron microscope (Hitachi Ltd., Japan). X-ray photoelectron spectroscopy (XPS) analysis was performed on a Thermo Scientific K-Alpha using Al Kα radiation. X-ray powder diffraction was performed on a Bruker D8 Advance diffractometer (40 kV, 40 mA) with Cu radiation (λ = 1.54056 Å) at room temperature. The dissolved oxygen meter is AR8010 (smart sensor). Confocal laser scanning microscopy studies were performed using a Leica TCS SP8 microscope (Germany). All electrochemical measurements were performed using an electrochemical workstation (CHI 660 D, Chenhua, China) in a three-electrode system consisting of a platinum wire counter electrode, Ag/AgCl reference electrode, and working electrode. PEC measurements were carried out on an electrochemical workstation (CHI 660 D) at room temperature using a conventional three-electrode cell. The light source was an Xe 300 W lamp (7IPX5002, Beijing Saifan) with an AM 1.5 G filter, and the light intensity at the WE was calibrated to 100 mW cm^{-2}. The potential value was recorded by the Ag/AgCl reference electrode, and the Nernst equation was used to convert the applied potential of the Ag/AgCl electrode to the potential of the reversible hydrogen electrode (RHE):

$$E_{RHE} = E_{Ag/AgCl} + E_{Ag/AgCl}(\text{reference}) + 0.0591V \times pH$$

where RHE E refers to the converted potential versus RHE. The value of $E_{Ag/AgCl}(reference)$ is 0.1976 V at ambient temperature (25 °C) and $E_{Ag/AgCl}$ is the obtained potential versus Ag/AgCl.

1.2. Preparation of the electrodes

Pretreatment of the FTO: In order to remove impurities such as grease and dust from the surface of the FTO, a sequential cleaning process was performed. FTO was sequentially placed in acetone, absolute ethanol and deionized water for ultrasonic 30 min, and the clean FTO was dried by nitrogen for further use.

Pretreatment of the carbon cloth: The carbon cloth was cut into 1 cm × 1.5 cm, cleaned with ethanol and deionized water three times, and dried in an oven at 40 °C.

Carbon nanotube substrate (SWCNT film) fabrication: Grinding SWCNT was mixed with 30% PTFE emulsion to control the mass ratio of SWCNT to PTFE was 85:15, which was rolled out into SWCNT film and set aside. The mass loading of the carbon nanotube film was 0.6 mg cm^{-2}.

1.3 X-ray diffraction for Au/$BiVO_4$/Si

In order to distinguish the substrate peak of FTO (37.76°) from the Au (111) (38.18°) crystal plane, Au/$BiVO_4$ was ultrasonically exfoliated from the FTO substrate and dropped onto the silicon wafer to confirm the existence of the Au (111) crystal plane peak.

1.4 Mott-Schottky analysis

The Mott-Schottky curve (M-S) test is an important means of characterizing the flat band potential (E_{fb}) as well as the carrier concentration (N_d). The slope of the

Mott-Schottky curve can be used to estimate the carrier concentration and is calculated as follows[1]:

$$N_d = \frac{2}{e\varepsilon\varepsilon_0}\left\{\frac{d\left(\frac{1}{C^2}\right)}{dV}\right\}^{-1}$$

Where e represents the electronic charge, with a value of 1.6×10^{-19} C, ε is the dielectric constant of the semiconductor, and $BiVO_4$ semiconductor material has a value of 68, ε_0 is the vacuum dielectric constant, which is 8.854×10^{-12} F/m, C is the space charge capacitance, V is the applied voltage, and $d(1/C^2)/dV$ is the slope of the Mott Schottky diagram. Additionally, the flat band potential (Efb) can be derived by extrapolating the X-intercept within the linear region of the M-S diagram[2].

1.5 Calculation of E_{CB}, E_{VB}

We can calculate the conduction band energy (E_{CB}) of the semiconductor according to Formula 1 based on the flat band potential value obtained by the M-S curve.[3]

$$E_{CB} = E_{fb} - 0.2 \quad (1)$$

Consequence, utilizing following Formula 2, we computed the respective valance band energy (E_{VB}) of the catalyst.

$$E_{VB} = E_g + E_{CB} \quad (2)$$

1.6 Glucose assay

The glucose concentration in the solution was determined using the 3,5-dinitrosalicylic acid (DNS) method[4]. Under alkaline conditions, the DNS reagent reacts with reducing sugar to produce brown-red 3-amino-5-nitrosalicylic acid. Within

a particular range, the depth of brown-red is related to the amount of reducing sugar in the sample. DNS (0.65 g) was dissolved in a small amount of hot water, then 2 mol/L NaOH (32.5 mL), propanetriol (4.5 g) was added, and finally, the solution was fixed to 100 mL with a secondary water. The above solution was stored in a brown bottle in a dark place for use.

For glucose assay, 600 μL of DNS reagent was added to 200 μL standard or sample, and the reaction was carried out at 95 ℃ for 5 min. The reaction was blocked by cold water, and the assay was completed in 10 min using a microplate reader.

1.7 Kinetic study of the photoelectrochemical oxidation for glucose

Glucose photoelectrochemical oxidation was carried out in a customized quartz electrolytic cell containing 10 mL of 2 mM glucose solution with 0.2 M PB (pH 7.4) as the supporting electrolyte. A typical three-electrode system was assembled using the prepared Au, $BiVO_4$ and Au/$BiVO_4$ electrode (working area 2 cm^2) as the working electrode, Ag/AgCl (3 M KCl) as the reference electrode, and Pt wire as the counter electrode. A Xe lamp (Saifan optoelectronic) with an optical filter (420 nm ≤ λ ≤ 780 nm) was employed as the light irradiation source. Prior to decomposition, the glucose solution was stirred for 30 min in the dark to achieve an adsorption-desorption balance. For the oxidation of glucose, we applied a constant voltage of 0.3 V and took samples at hourly intervals, ending the reaction after 6 hours.

1.8 The measurement of dissolved oxygen

O_2 produced in the photocatalytic water decomposition reaction was recorded by a portable dissolved oxygen meter. The dissolved oxygen meter was placed in a

sealed quartz cell under light and O_2 concentrations were recorded at regular intervals in the PB buffer containing glucose or not.

1.9 The test of electrochemical impedance spectroscopy (EIS)

The electrolyte for the EIS tests was a solution containing 0.5 M potassium ferricyanide and 0.5 M potassium ferrocyanide. A three-electrode system was employed, with either a $BiVO_4$ or Au/$BiVO_4$ photoanode as the working electrode, a platinum wire as the counter electrode, and an Ag/AgCl reference electrode. The frequency range was set from 0.01 Hz to 100 kHz, with an amplitude of 5 mV.

2 Supporting Figures

Figure S1

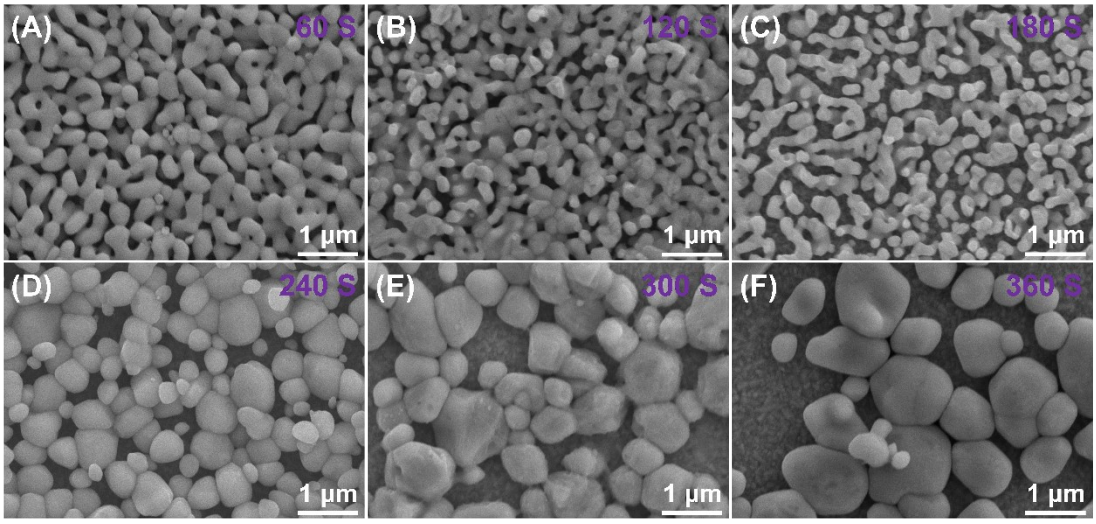

Fig. S1. SEM images of $BiVO_4$ obtained by different electrodeposition time for BiOI (A) 60 s, (B) 120 s, (C) 180 s, (D) 240 s, (E) 300 s, (F) 360 s.

Figure S2

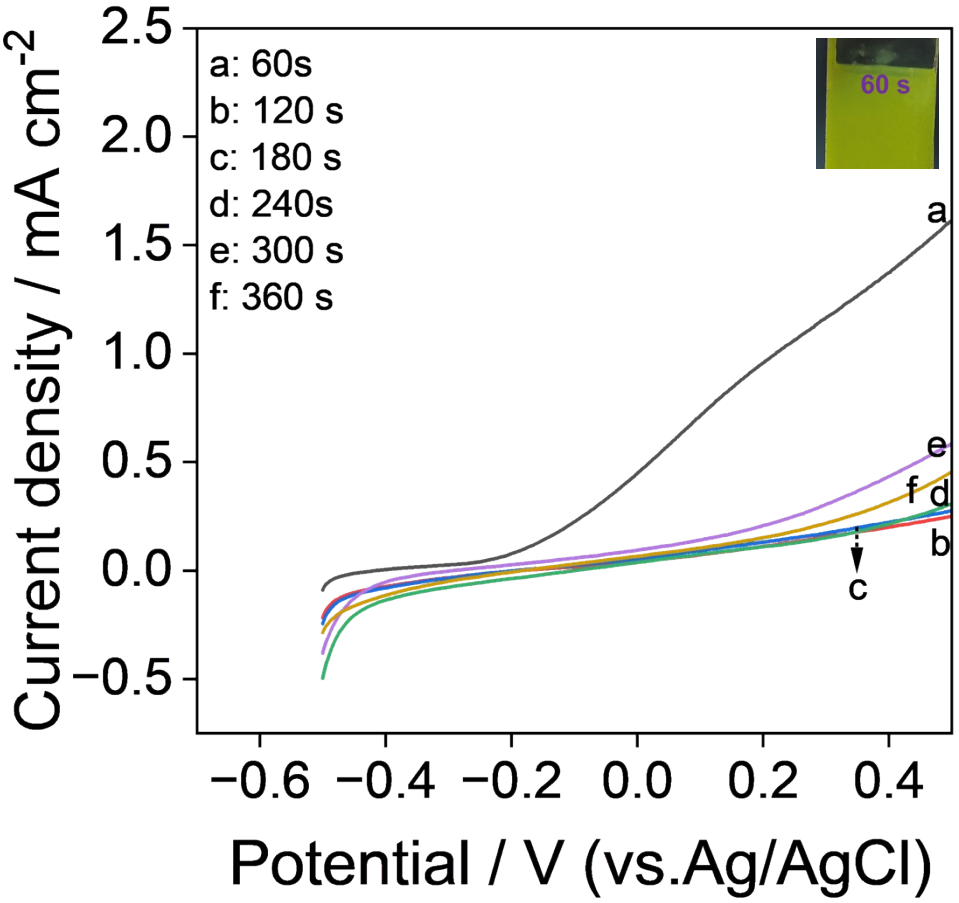

Fig. S2. LSV response of $BiVO_4$ synthesized by different electrodeposition times in 0.2 M PB (pH 7.4) containing 200 mM glucose. All LSVs are scanned at 50 mV s^{-1}.

Figure S3

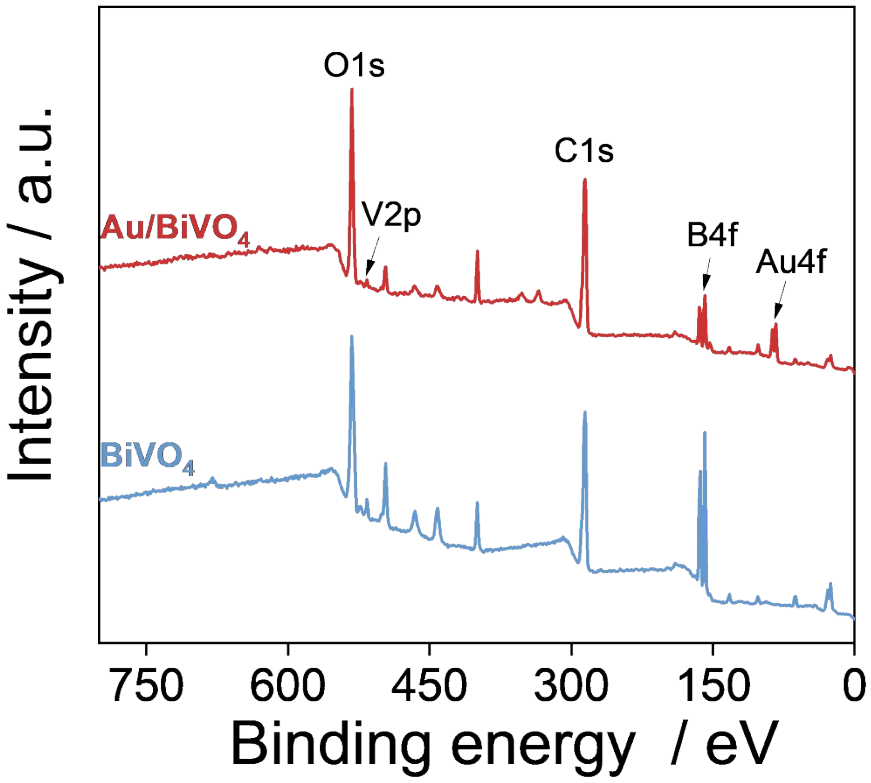

Fig. S3. XPS spectra of $BiVO_4$, $Au/BiVO_4$.

Figure S4

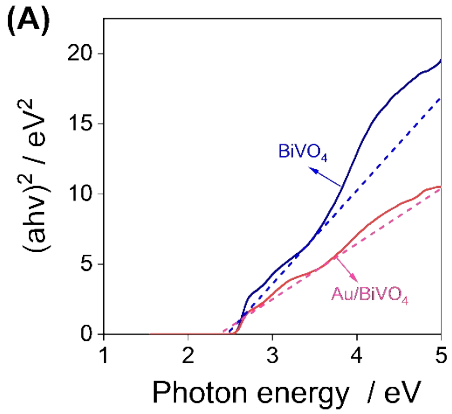

(B)

Material	E_g	E_{CB} (vs RHE)	E_{VB} (vs RHE)
$BiVO_4$	2.45 eV	0.04 eV	2.49 eV
$Au/BiVO_4$	2.36 eV	-0.15 eV	2.21 eV

Fig. S4. (A) Tauc plots and (B) band gap (E_g), valence band (E_{VB}) and conduction band (E_{CB}) data of $BiVO_4$, $Au/BiVO_4$.

Figure S5

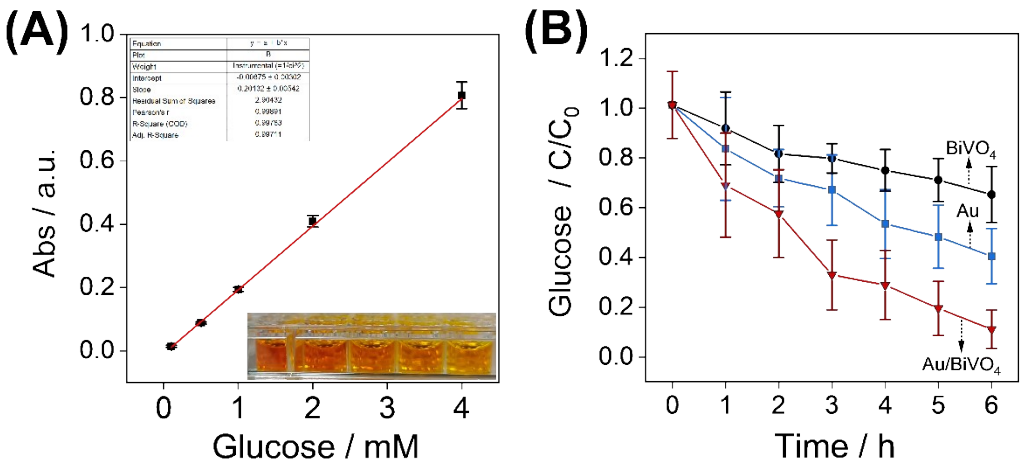

Fig. S5. (A) Calibration curve for the UV-Vis absorbance at 530 nm wavelength of DNS solution in the concentration ranging from 0 to 4 mM. (B) Au, $BiVO_4$ and $Au/BiVO_4$ electrode for glucose oxidase at 0.3 V.

Figure S6

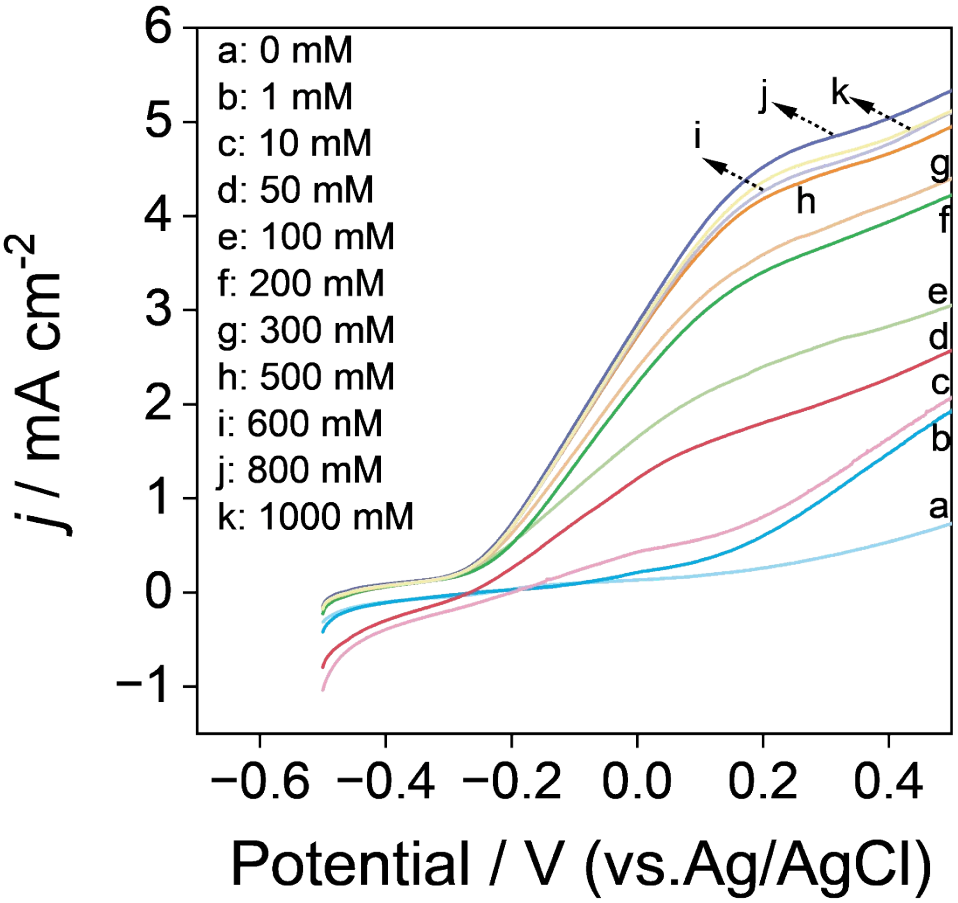

Fig. S6. LSV curves of $Au/BiVO_4$ electrode measured in 0.2 M PB (pH 7.4) with different glucose concentrations. All LSVs are scanned at 50 mV s^{-1}.

Figure S7

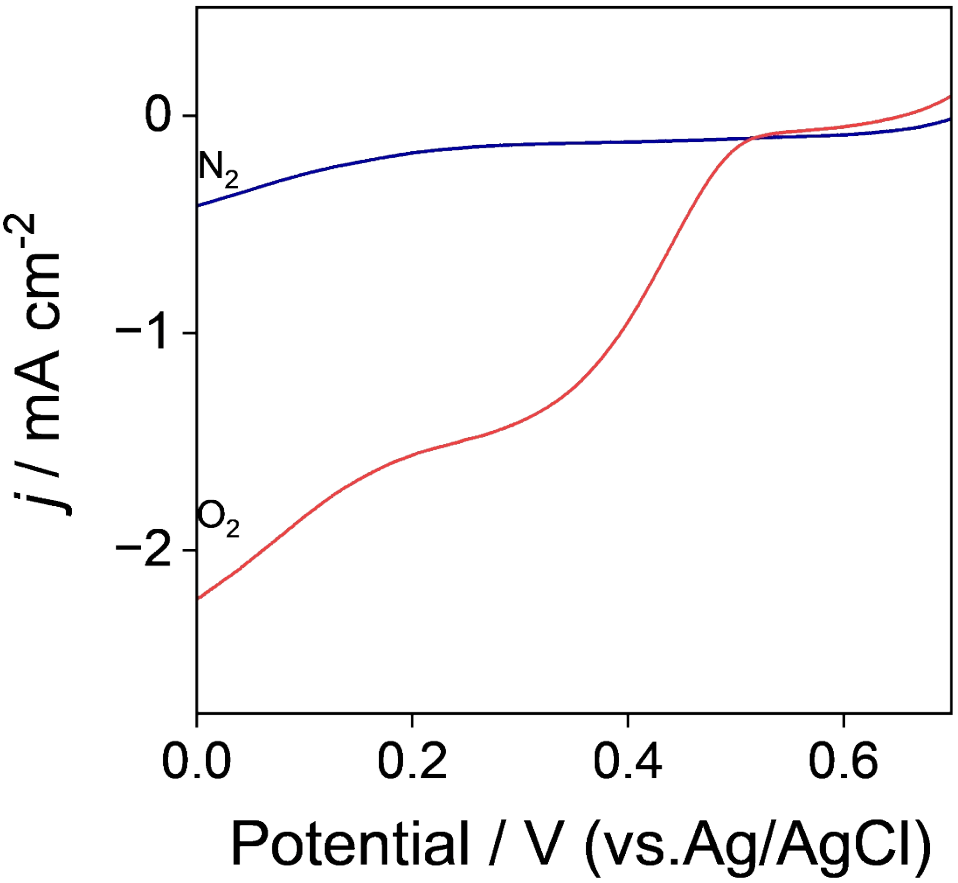

Fig. S7. LSVs of the BOD/SWCNT biocathode in 0.2 M PB (pH = 7.4) saturated with N_2 (blue curve) and O_2 (red curve). All LSVs are scanned at 50 mV s^{-1}.

Figure S8

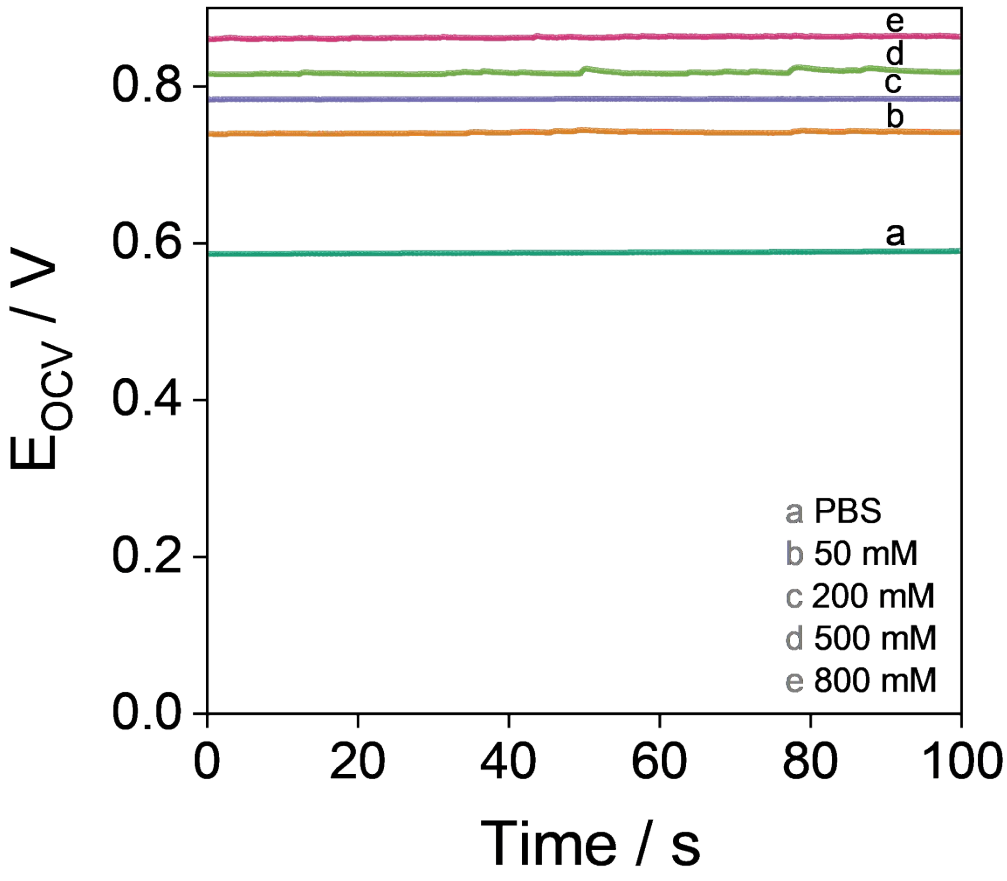

Fig. S8. The Eocv of the GBFC with irradiation correspond to glucose concentrations of 0, 50, 200, 500, and 800 mM.

Figure S9

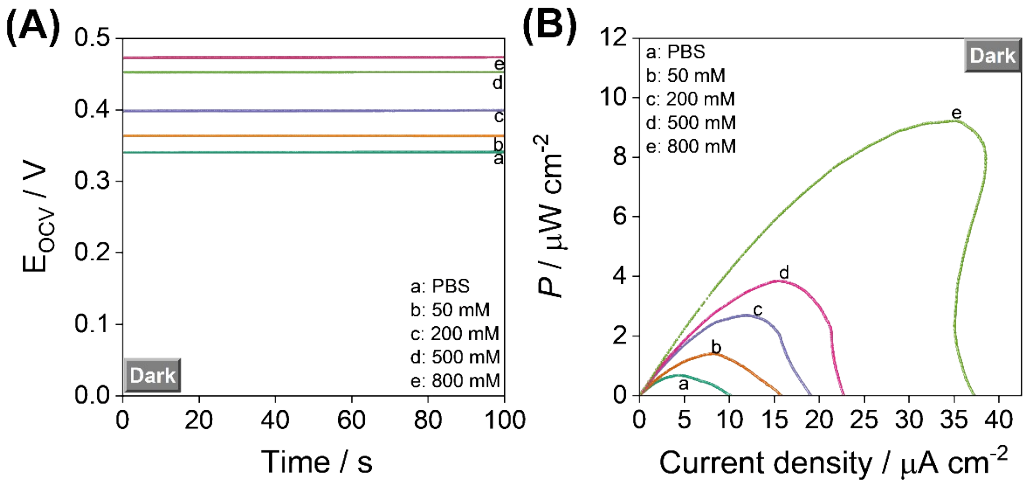

Fig. S9. (A) E_{ocv} and (B) power densities of the GBFC without irradiation corresponding to 0, 50, 200, 500 and 800 mM glucose. Scan rate: 1 mV s^{-1}.

Figure S10

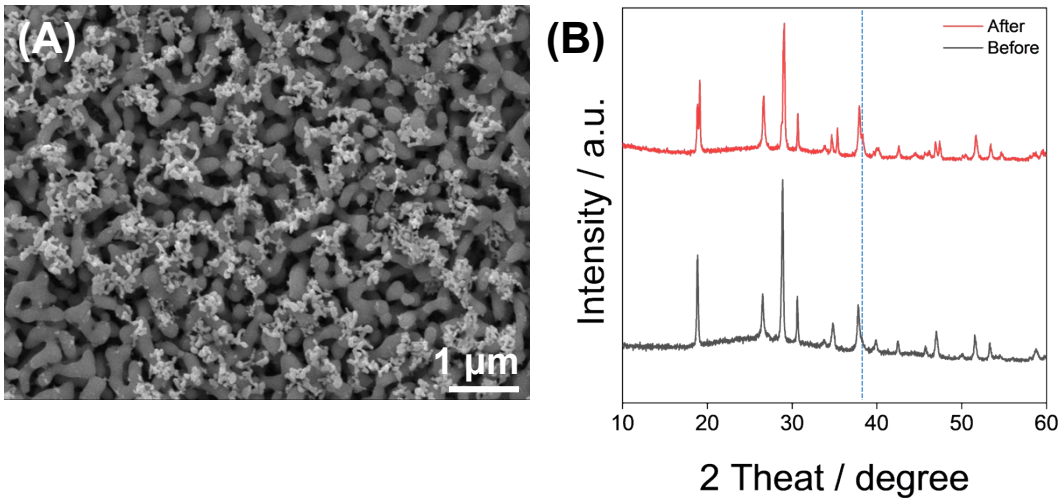

Fig. S10. (A) XRD and (B) SEM images of anodic Au/$BiVO_4$ after GBFC discharge for 20 h.

3 Supporting Tables

Table S1

Glucose/O_2 fuel cell anode performance comparison under a neutral environment

Anode	Electrolyte	Glucose oxidation current (0.5 V)	Glucose concentration	References
Rhodium single-atom (Rh SANs)	PBS (0.1 M pH 7.4)	1.75 mA cm^{-2}	100 mM	ACS Energy Lett., 2023, 8, 1697-1704
CuO/MWCNTs-PEDOT: PSS	PBS (0.1 M pH 7.4)	≈ 0.012 mA	10 mM	Adv. Mater., 2023, 35, 2300890
Pt Nanoflowers (Pt NFs)	PBS (0.1 M pH 7.4)	3 mA cm^{-2}	5 mM	ACS Appl. Mater. Interfaces, 2023, 15, 17969-17977
PdAuNS/f-CNT/SPCE	PBS (0.1 M pH 7.4)	≈ 0.8 mA	20 mM	Biosens. Bioelectron., 2022, 210, 114335
Pt/Au nano-alloy/ Pt@PETE	PBS (0.1 M pH 7.4)	≈ 0.2 mA	5 mM	J. Power Sources, 2021, 486, 229374
AuNWs/GCE	PBS (0.1 M pH 7.4)	≈ 0.15 mA cm^{-2}	30 mM	Biosens. Bioelectron., 2014, 52, 105-110
Al/Au/ZnO	PBS (0.1, pH 7.4)	≈ 0.1 mA	25 mM	J.Power Sources, 2014, 261, 332-336
AuNW	PBS (0.1 M pH 7.4)	≈ 0.4 mA cm^{-2}	5 mM	Energy Environ. Sci., 2013, 6, 3600-3604
Pt-Au alloy nanoparticles	PBS (0.1 M pH 7.4)	≈ 0.7 mA cm^{-2}	100 mM	J. Phys. Chem. B, 2007, 111, 10329
Au/$BiVO_4$	PB (0.2 M pH 7.4)	5.33 mA cm^{-2}	800 mM	This work

Table S2

Performance comparison of glucose/O_2 biofuel cells based on glucose oxidase (GOD or GOx) anodes

Anode	Cathode	Electrolyte conditions	Performance	Reference
Ti_3C_2Tx/MWCNTs/AuNPs /GOx	$ZnCo_2$@NCNT	0.1 M PBS containing 5 mM glucose	Stability: N/A; Eocv = 0.497 V; Pmax = 61.34 μW cm^{-2}	Small, 2023, 19, 2206257
BP/[TTF-GOx]/Gelatin-GA	BP/4-APA/BOD	0.01 M PBS (pH 7.0) containing 0.01 M glucose	Stability: N/A; Eocv = 0.61 V; Pmax = 92 μW cm^{-2}	Appl. Energ., 2023, 339, 120978
GRE/PPD/(AuNPs)PPCA-GOx	GRE/PB-PPCA/PPCA–GOx	APS-KCl (pH 6.0) containing 40 mM glucose	Stability: 36 days, 90%; Eocv = 0.63 V; Pmax = 10.94 μW cm^{-2}	Biosens. Bioelectron., 2022, 216, 114657
GOx/rGO/FP	Lac/rGO/FP	0.01M PBS (pH 7.4) containing 40 mM glucose	Stability: N/A; Eocv = 0.04 V; Pmax = 4.0 nW cm^{-2}	ACS Appl. Mater. Interfaces, 2022, 14, 24229-24244
GR/PB-PPCA/PPCA-GOx	GR/PB-PPCA/PPCA-GOx	A-PBS-KCl (pH 6.0) containing 10 mM glucose	Stability: 14 days, 95%; Eocv = 0.15 V; Pmax: N/A	Sci. Rep., 2021, 11, 18568
GOx/[FeCo-OMPC/CNT]	FeCo-OMPC	0.02 mM PBS (pH 7.4) containing 30 mM glucose	Stability: N/A; Eocv = N/A; Pmax = 1.2 μW cm^{-2}	Appl. Surf. Sci., 2020, 511, 145449
NPG/Os(bpy)PVI/GOx	CPG/RGO-A/BOD	0.1 M PBS (pH 7.0) containing 20 mM glucose	Stability: N/A; Eocv = 0.51 V; Pmax = 22 μW cm^{-2}	Biosens. Bioelectron., 2020, 167, 112500
GOx/Porous structured carbon paper	Lac/Porous structured carbon paper	0.1 M PBS (pH 7.4) containing 5 mM glucose	Stability: 2000 s, 75%; Eocv = 0.60 V; Pmax = 9.64 μW cm^{-2}	J. Mater. Chem. B, 2020, 8, 3550-3556

GOx/Cross-linking of chitosan and genipin	Lac	0.01 M PBS (pH7.4) containing 20 mM glucose	Stability: N/A; Eocv = 0.54 V; Pmax = 38 μW cm^{-2}	ACS Appl. Mater. Interfaces, 2020, 12, 23635-23643
RPPy/GOx	Lac	acetate buffer (pH 5.0) containing 0.05 M glucose	Stability: N/A; Eocv = 1.16 V; Pmax = 350 μW cm^{-2}	Biosens. Bioelectron., 2019, 132, 76-83
MGCE/Fe_3O_4-RGO/GOx	MGCE/Fe_3O_4-RGO/BOD	0.1 M PBS (pH 7.0) containing 5 mM glucose	Stability: N/A; Eocv = 0.626 V; Pmax = 73.7 μW cm^{-2}	Sci. Rep., 2017, 7, 12882
Au/$BiVO_4$	BOD	PB (0.2 M, pH = 7.4) with 800 mM glucose	Stability 20 h, 80 %; Eocv = 0.86 V; Pmax = 575 μW·cm^{-2}	This work

Table S3

Performance comparison of glucose oxygen biofuel cells based on photoelectrocatalytic anodes

Anode	Cathode	Electrolyte conditions	Performance	Reference
$BiVO_4$	Hemin/BP	0.1M PBS (pH 7.0) with 10 mM glucose	Stability 12 h; Eocv = 0.62 V; Pmax = 139.17 μW·cm $^{-2}$	Appl. Catal. B-Environ. Energy, 2024, 343, 123481.
TiO_2/TCPP/GDH	MCHS/CP	Tris-HCl (0.25 M, pH 8.0) + NAD^+ (10 mM) with 120 mM glucose	Stability 3 h, 73%; Eocv = 0.76 V; Pmax = 240 μW·cm $^{-2}$	J. Mater. Chem. A, 2023, 11, 600-608.
Mo: $BiVO_4$	GOD/PB	0.1 M PB (pH 6.0) containing 60 mM glucose	Stability: N/A; Eocv = 0.508 V; Pmax = 170.35 μW cm^{-2}	Nano Energy, 2022, 104, 107940.
$BiVO_4$	Pt	0.2 M NaBi containing 20 mM glucose	Stability: N/A; Eocv = 0.56 V; Pmax = 24.9 μW cm^{-2}	Electroanal. Chem., 2021, 882, 114912
TiO_2-PbS QD/Os CP/GDH	GOx/PEI/$BiFeO_3$	PBS (0.05 M, pH = 7.0) with 100 mM glucose	Stability 20 min, 70%; Eocv =1.0 V; Pmax =10 μW·cm^{-2}	Angew. Chem. Int. Ed., 2021, 60, 2078-2083.
Fe_2O_3	Pt	1 M NaOH containing 2.5 mM glucose	Stability: N/A; Eocv = N/A; Pmax = 8.0 μW cm^{-2}	Sensors & Actuat. B. Chem., 2020, 310, 127842.
TNA/A-g-C_3N_4	CBFeO (Fe^{3+}-doped $CuBi_2O_4$)	0.1 M PB (pH 7.4) containing 10 mM glucose	Stability: N/A; Eocv = 0.98 V; Pmax = 133.5 μW cm^{-2}	Biosens. Bioelectron., 2020, 165, 112357.
AuNP/g-C_3N_4	BOD	0.1 M PB (pH 7.4) containing 0.1 M glucose	Stability: N/A; Eocv = 0.508 V; Pmax = N/A	J. Mater. Chem. B, 2019,7, 2277-2283.
Au-TiO_2 NRAs	pTTh-Cu_2O	0.1 M (PBS) (pH 7.0) containing 50 mM glucose	Stability: 8 h, 40%; Eocv = 0.78 V; Pmax = 130 μW·cm^{-2}	Appl. Catal. B-Environ. Energy, 2019, 250, 171-180

TiO_2	Pt	1 M NaOH containing 0.05 mM glucose	Stability: N/A; Eocv = N/A; Pmax = 140 μW cm^{-2}	Electrochem. Commun., 2018, 94, 18-22
W: $BiVO_4$	pTTh	sodium borate containing 0.10 M glucose	Stability: 20 h, 50% Eocv = 0.62 V; Pmax = 82 μW cm^{-2}	ChemSusChem., 2017, 10, 99-105
$Ni(OH)_2/CdS/TiO_2$	hemin-graphene (HG	0.1 M PB (pH 7.4) containing 500 μM glucose	Stability: N/A; Eocv = N/A; Pmax = 28 μW cm^{-2}	Anal. Chem. 2016, 88, 12, 6140-6144
TiO_2	Pt wire	0.1 M Na_2SO_4 (pH 5.9) containing 10 mM glucose	Stability: N/A; Eocv = 0.57 V; Pmax = 4.81 μW cm^{-2}	Chem. Commun., 2013, 49, 8632-8634
$Au/BiVO_4$	BOD	PB (0.2 M, pH = 7.4) with 800 mM glucose	Stability 20 h, 80 %; Eocv = 0.86 V; Pmax = 575 μW·cm^{-2}	This work

4. Supplementary References

1. S. Qu, H. Wu and Y. H. Ng, *Small*, 2023, **19**, 2300347.

2. H. Wang, R. Gao, N. T. Nguyen, J. Bai, S. Ren, X. Liu, X. Zhang and L. Wang, *ACS Nano*, 2023, **17**, 22071-22081.

3. L. Gao, Y. Zhou, L. Cao, X. Cui, Y. Zheng, H. Yin and S. Ai, *Anal. Chem.*, 2022, **94**, 16936-16944.

4. Y. Li, R. Fu, Z. Duan, C. Zhu and D. Fan, *Small*, 2022, **18**, 2200165.